JOURNAL OF COMPUTATIONAL PHYSICS 63, 363–376 (1986)

Absorbing Boundaries for Wave Propagation Problems

R. KOSLOFF

Department of Physical Chemistry and the Fritz Haber Center for Molecular Dynamics, Hebrew University, Jerusalem, Israel

AND

D. KOSLOFF

Department of Geophysics and Planetary Sciences, Tel Aviv University, Tel Aviv, Israel

Received May 22, 1984; revised April 1, 1985

Reflections or wraparound from boundaries of numerical grids have always presented a difficulty in applying discrete methods to simulate physical phenomena. This study presents a systematic derivation of absorbing boundary conditions which can be used in a wide class of wave equations. The derivation is applied to the Schrödinger equation and to the acoustic equation in one and two dimensions. The effectiveness of the absorbing boundary conditions can be evaluated apriori on the basis of analytic solutions.

I. INTRODUCTION

In the numerical simulation of wave propagation by spatially discrete methods, there is always a need to eliminate spurious events which are generated by the boundaries of the numerical grid. These events arise because the numerical mesh covers a finite region of space. The boundary effects can appear as reflections as in the finite difference method or as wraparound in the Fourier method. These events are always extraneous to the real physical events under study so that their elimination is desirable.

In this study a systematic method to eliminate the boundary events through the application of absorbing boundaries is presented. The method is applied to the Schrödinger and acoustic wave equations. It is based on a simple modification of the wave equation so that the wave amplitude becomes attenuated at the grid boundary region. This method is an extension of one developed previously on empirical grounds for the acoustic and elastic wave equations [1]. In the previous study an absorbing boundary was achieved through a gradual elimination of the wave amplitude in a strip along the boundary of the grid. The present paper derives the absorbing boundaries in a consistent fashion. This allows a quantative analysis

0021-9991/86 $3.00

of the method and enables to apply it also with implicit and semi implicit time integration schemes.

The importance of absorbing boundaries has been recognized in the past and consequently a number of methods have been proposed for constructing absorbing boundaries [2–4]. Lysmer and Kuhlemeyer [2] proposed a method based on viscous damping on the boundaries of the numerical mesh. A class of methods derived more recently is based on replacing the wave equation on the boundary grid points by a one way equation which allows energy to propagate in the outward direction only [3, 4]. This method has proven effective for waves which impinge vertically on the boundary, however, the method usually degrades for grazing angles of incidence. It is also highly dependent on the type of wave equation and the spatial discretization method. For example, it is not obvious how to apply this boundary condition or the method described in [2] to spatially periodic methods such as the Fourier method used for this study.

Elimination of amplitude is also important in purely analytical calculations. In the field of photophysics and photochemistry for example, the excited state decays into the continuum. To describe such a phenomena a complex potential has been introduced (optical potential). This potential eliminates the amplitude of the excited states. It is later shown that the method of this study as applied to the Schrödinger equation is equivalent to introducing a complex negative potential in the absorbing region.

In the next section absorbing boundaries for the Schrödinger equation are first derived on an empirical basis. A similar method was used for the acoustic and elastic wave equations [1]. It is then shown that the method can be reformulated as a special solution scheme for the Schrödinger equation with a complex optical potential. The new formulation is applied to the Chebychev propagation scheme [5]. In Section III the same theory is applied to the acoustic wave equation.

II. Absorbing Boundaries for the Fourier Solution Method to the Schrödinger Equation

In quantum mechanics the state of the system is represented by the wave function ψ, while the time evolution is governed by the Schrödinger equation

$$i\frac{\partial \Psi}{\partial t} = \hat{H}\Psi, \tag{2.1}$$

where $\hat{H}$ is the Hamiltonian of the system: $\hat{H} = -(\hat{\nabla}^2/2m) + \hat{V}$. In the Fourier method the spatial derivatives are calculated with the use of the FFT algorithm [6–8] and the solution is propagated by second-order differencing.

Use of the Fourier method implies periodic boundary conditions. Figure 1a demonstrates the consequences of this numerical phenomena where the wavefunction wraps around and appears at the other side of the grid. Conversely by

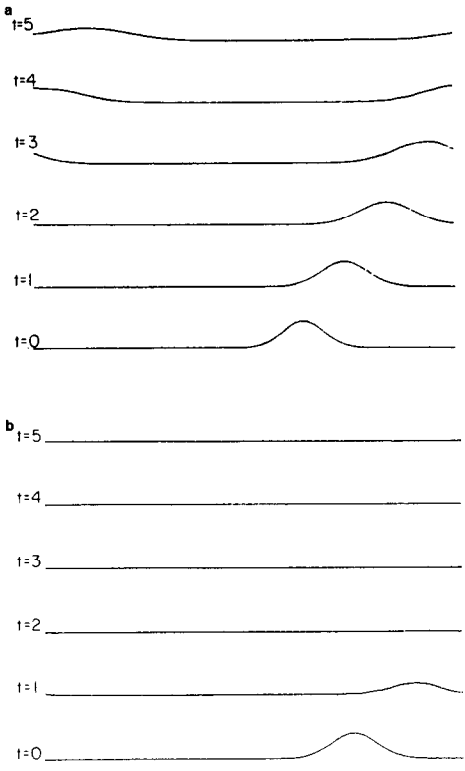

FIG. 1. A one-dimensional Schrödinger wave equation solution by the Fourier method (a) without absorbing boundaries at successive times, (b) with absorbing boundaries.

using a strong repulsive potential the periodic boundaries are replaced by reflecting boundaries. None of these conditions can simulate the physical behaviour of an unbounded potential free region.

In the previous work [1] it was found that an absorbing boundary can be obtained by a gradual reduction of amplitude at the end of each time step. This reduction takes place in a strip of grid points surrounding the mesh. The reduction factor has the largest value on the grid boundary and it tapers gradually towards the center of the grid. This gradual tapering is necessary to eliminate reflections. A similar procedure can be applied to the Schrödinger equation.

Let Ψ_n denote the wavefunction at the time step n. The following steps describe the propagation scheme for the Schrödinger equation which includes the absorbing part.

(a) Calculate the Hamiltonian operation $\hat{H}\Psi_n$ by using the FFT algorithm to calculate spatial derivatives. Next calculate the potential operation by multiplying Ψ_n by the potential $\hat{V}$.

(b) Time step according to

$$\Psi^{(0)}_{n+1} = \Psi_{n-1} + 2i\,dt\,\hat{H}\Psi_n, \qquad \text{with} \quad i = \sqrt{-1}. \tag{2.2}$$

(c) Amplitude reduction

$$\Psi_{n+1} = (1 - \gamma\,dt)\,\Psi^{(0)}_{n+1} \tag{2.3}$$

with γ denoting the reduction function.

Steps (a) and (b) have been used previously for solving the Schrödinger equation without absorbing boundaries [7, 8]. Step (c) is an additional forward differencing step for the amplitude elimination. Empirically it was found that for efficient absorption the derivative of γ should be kept as small as possible to avoid reflections. On the other hand, the value of γ should be large enough to eliminate transmission. In this work the following spatial dependence for γ was chosen,

$$\gamma = U_0/\cosh^2(\alpha \cdot n), \tag{2.4}$$

where U_0 is a constant, α is a decay factor and n denotes the distance in number of grid points from the boundary. The effect of the absorbing boundary is apparent in Fig. 1b which shows the same wavepacket propagation as in Fig. 1a but with the absorbing boundary. The wavepacket is completely eliminated, effectively mimicing an infinite region.

Close examination of the above empirical absorbing scheme, reveals that the function γ plays a similar role to a complex negative potential added to the Hamiltonian. The amplitude reduction step c can be derived from the equation

$$\frac{\partial \Psi}{\partial t} = -\gamma \Psi \tag{2.5}$$

with a first-order time propagation scheme. When Eq. (2.5) is added to the original Schrödinger equation (2.1), it becomes apparent that the absorbing function γ is merely a complex potential. In principle therefore, the absorbing boundary can be incorporated into one equation with a complex potential. However, a careful choice of a time integration scheme is required to ensure numerical stability.

Using the idea of a complex potential one can examine analytically the features needed for a good absorption. The one-dimensional Schrödinger equation with the potential

$$\hat{V}(x) = U_0/\cosh^2(\alpha x) \tag{2.6}$$

with U_0 real, is a well-known model potential for which the transmission and reflection coefficients have been worked out analytically [9]. For a complex potential

one can analytically continue the solutions to obtain the values of the transmission and reflection coefficients as a function of the wavenumber k,

$$T=\sqrt{(-ik-S)}\sqrt{(-ik+S+1)}/(\sqrt{(-ik)}\cdot\sqrt{(1-ik)},$$

and (2.7)

$$R=T\cdot\sqrt{(ik)}\cdot\sqrt{(1-ik)}/(\sqrt{(-S)}\cdot\sqrt{(1+S)})$$

with

$$S=\tfrac{1}{2}\,[\sqrt{1-(8mU_0/\alpha^2)}].$$

The constant U_0 in 2.7 is pure imaginary.

One should notice that in this case $|R|+|T|<1$. By varying U_0 and α in (2.6) one can optimize the absorbing potential. In this optimization a balance is chosen between the number of grid points used for the absorbing region, and a sufficient reduction of the amplitude for the wavenumbers contained in the wavepacket. Figure 2 displays the transmission and reflection coefficients as a function of

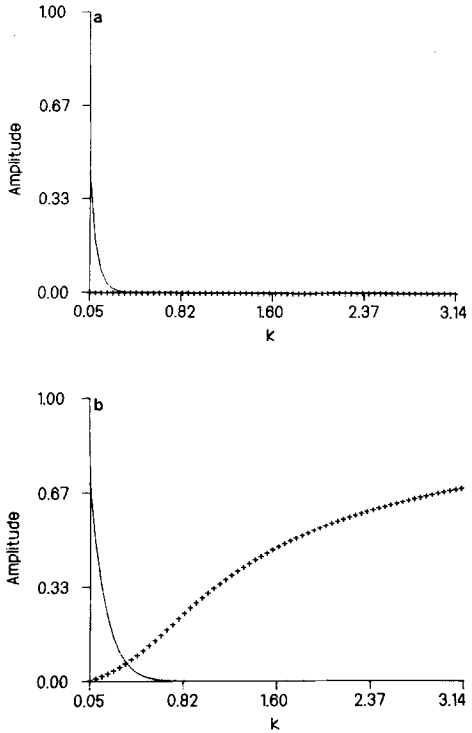

FIG. 2. Reflection and transmission coefficients of the absorbing region as a function of wavenumber for the complex potential (a) $\alpha=0.18$ and $U_0=0.02$ used in Fig. 1b, (b) $\alpha=0.5$ $U_0=0.001$.

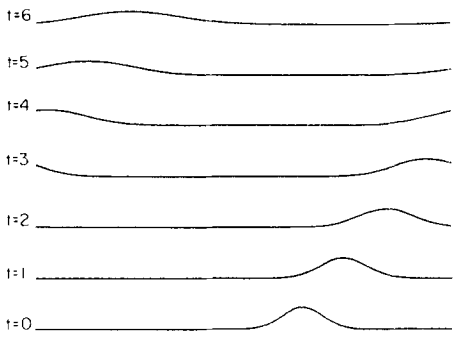

FIG. 3. A one-dimensional Schrödinger wave equation solution by the Fourier method with absorbing boundaries with the parameters of Fig. 2b.

wavenumber k for the potential given in (2.6). Figure 2a displays R and T for the absorbing parameters used in Fig. 1b. Conversely Fig. 2b examples a poor choice of absorbing parameters with the transmission coefficient too high. Figure 3 shows results of propagation with this poor choice of parameters. These simple one-dimensional examples show the important features of the absorbing boundary. Similar results are also found in physically more interesting multidimensional problems.

Once the absorbing boundary has been identified as a complex potential it can also be used to set up absorbing boundaries for semi implicit propagation schemes. The Chebychev propagation scheme [5] has been found stable, provided the complex contribution to the eigenvalues of the Hamiltonian are relatively small. This fact has important significance since the semi-implicit Chebychev method has proven to be very accurate and efficient for scattering problems with static potentials [5, 10].

Figures 4a–e demonstrates the application of such absorbing boundaries for simulating the reactive scattering of $H + H_2$. The propagation scheme used was the Chebychev method [5]. The width of the absorbing strip was twenty grid points. The absorbing boundary eliminated the amplitude of the reactive part, mimicing an infinite scattering region. Figure 4f displays the same propagation event without absorbing boundaries. The result is that the wave reaches the boundary and is reflected from the repulsive potential connected through the periodic boundary conditions.

III. Absorbing Boundary Condition for the Acoustic Wave Equation

An absorbing boundary for the acoustic wave equation can be derived by the same steps used for the Schrödinger equation. For the sake of brevity, derivation using the empirical approach is not repeated since it was previously described [1]. We now can proceed to describe the modified absorbing acoustic equation. Con-

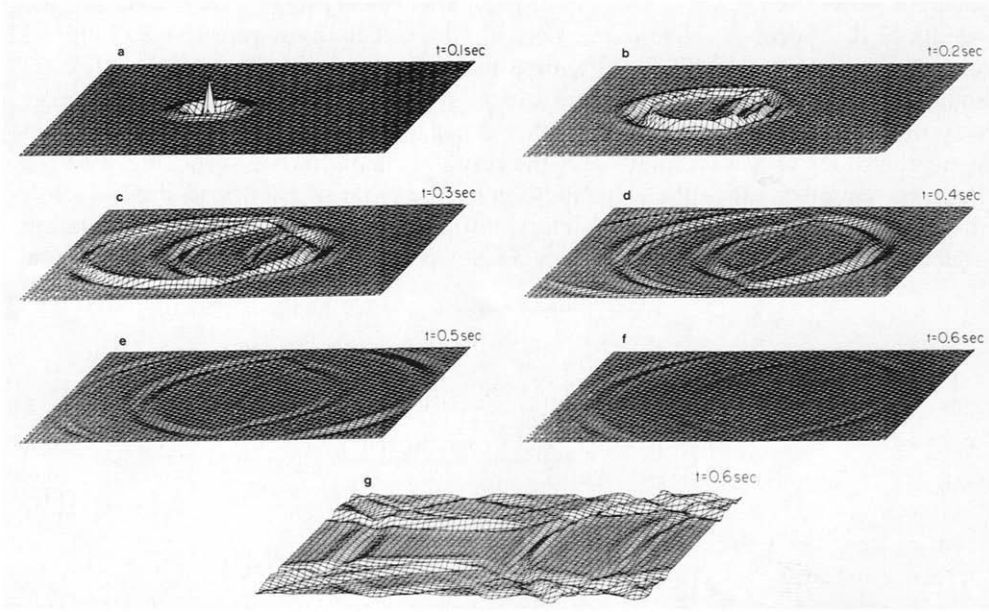

FIG. 4. A two-dimensional Schrödinger wave equation for the collinear reaction $H + H_2$ with absorbing boundaries propagated by the Chebychev scheme at successive times. (f) The snapshot at time $t = 5000$ without absorbing boundaries.

sider a two-dimensional acoustic medium with a variable density $\rho(x, y)$ and acoustic velocity $c(x, y)$. Wave motion in the medium is governed by the acoustic wave equation given by

$$\frac{\partial}{\partial x}\left(\frac{1}{\rho}\frac{\partial p}{\partial x}\right)+\frac{\partial}{\partial y}\left(\frac{1}{\rho}\frac{\partial p}{\partial y}\right)=\frac{1}{\rho c^2}\frac{\partial^2 p}{\partial t^2}+S(x, y, t). \tag{3.1}$$

P represents the pressure, S is a source term, and x, y are Cartesian coordinates. To follow the same steps used for the Schrödinger equation, Eq. (3.1) is rewritten as two coupled first-order differential equations in time,

$$\frac{\partial}{\partial t}\begin{bmatrix} p \\ V \end{bmatrix}=\begin{bmatrix} 0 & 1 \\ \rho c^2\left(\dfrac{\partial}{\partial x}\left(\dfrac{1}{\rho}\dfrac{\partial}{\partial x}\right)+\dfrac{\partial}{\partial y}\left(\dfrac{1}{\rho}\dfrac{\partial}{\partial y}\right)\right) & 0 \end{bmatrix}\begin{bmatrix} p \\ V \end{bmatrix}+\begin{bmatrix} 0 \\ S' \end{bmatrix} \tag{3.2}$$

with $S' = \rho c^2 S$.

The first equation in (3.2) expresses the relation $V = \partial p/\partial t$, whereas the second

equation is identical to (3.1). In analogy to the Schrödinger equation, the absorbing boundary condition is achieved by replacing (3.2) with the system

$$\frac{\partial}{\partial t}\begin{bmatrix} p \\ V \end{bmatrix} = \begin{bmatrix} -\gamma & 1 \\ \rho c^2 \left(\frac{\partial}{\partial x}\left(\frac{1}{\rho}\frac{\partial}{\partial x}\right) + \frac{\partial}{\partial y}\left(\frac{1}{\rho}\frac{\partial}{\partial y}\right) \right) & -\gamma \end{bmatrix} \begin{bmatrix} p \\ V \end{bmatrix} + \begin{bmatrix} 0 \\ S' \end{bmatrix}. \tag{3.3}$$

The parameter γ plays the role which the optical potential played in the Schrödinger equation. The first-order system (3.3) can serve as a basis for time integration. For the absorbing boundary the parameter $\gamma(x, y)$ differs from zero only in a strip of nodes surrounding the numerical mesh. As with the Schrödinger equation, the spatial dependence of γ is chosen to achieve the best amplitude elimination.

In constructing numerical schemes it sometimes may be more convenient to work with a single second order equation. This equation is obtained from (3.3) after elimination of the variable V giving

$$\frac{\partial^2 p}{\partial t^2} = \rho c^2 \left(\frac{\partial}{\partial x}\left(\frac{1}{\rho}\frac{\partial p}{\partial x}\right) + \frac{\partial}{\partial y}\left(\frac{1}{\rho}\frac{\partial p}{\partial y}\right) \right) + S' - 2\gamma \frac{\partial p}{\partial t} - \gamma^2 p. \tag{3.4}$$

Equation (3.4) can be integrated in time with a suitable stable time differencing scheme.

The success of the absorbing boundary can be understood by considering one-dimensional wave propagation when all the variables are constant in space, and the source term is zero. Equation (3.4) then reads

$$\frac{\partial^2 p}{\partial t^2} = c^2 \frac{\partial^2 p}{\partial x^2} - 2\gamma \frac{\partial p}{\partial t} - \gamma^2 p. \tag{3.5}$$

This equation possesses a general solution of the form

$$p(x, t) = Af_1(x - ct)\, e^{-(\gamma/c)x} + Bf_2(x + ct)\, e^{(\gamma/c)x} \tag{3.6}$$

with A and B arbitrary constant and f_1 and f_2 arbitrary twice differentiable functions. This solution represents travelling waves which are exponentially attenuated in space. All frequency components are equally attenuated because the decay factor γ/c is frequency independent. This fact has important significance, as a propagating pulse containing a frequency band will gradually attenuate without changing shape or undergoing dispersion.

When the decay factor γ is spatially variable, Eq. (3.4) can be solved by the propagator matrix method (Appendix). The effectiveness of the absorbing region can thus be evaluated numerically. Consider one-dimensional wave propagation in a region $-\infty < x < \infty$. The acoustic velocity is uniform and the absorbing coefficient γ differs significantly from zero only in the region $a < x < b$. A sinosoidal

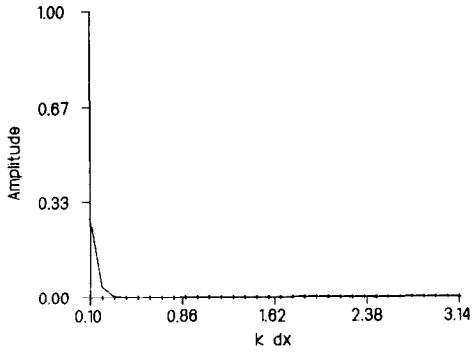

FIG. 5. Reflection and absorbing coefficients of the absorbing region for the acoustic wave equation with $c = 2000$ m/sec, $\alpha = 0.18$ $U_0 = 40$.

wave $\exp(i(wt - kx))$ in the region $-\infty < x < a$, and with $w/k = c$ creates a reflected wave $R \exp(i(wt + kx))$ for $x < a$, and a transmitted wave $T \exp(i(wt - kx))$ for $b < x$. When the spatial dependence of γ is chosen properly, the magnitude of T and R can be kept small thus effectively ensuring that no energy is reflected or transmitted from the absorbing region.

In this study the spatial dependence of γ, given in (3.4) was again chosen. The choice has proven successful although other relations may work out equally well. The magnitude of the reflection coefficient R and the transmission coefficient T, for different wavenumbers is shown in Fig. 5. The calculations were based on the results of the Appendix. The parameters for the calculations were $C = 2000$ m/sec, $U_0 = 40$ sec^{-1} and $\alpha = 0.18$ m^{-1}. Figure 5 shows that the magnitude of T and R are small for this choice of parameters except at the extremes of small and large wavenumbers. For the small wavenumber range, the width of the absorbing region is on the order of a wavelength and the result therefore is not surprising. For the large wavenumber range the wavelength is on the order of a few grid sizes which is also the order of the discretization interval of the parameter α. In actual calculation which use band limited sources which do not contain wavelengths in the extreme

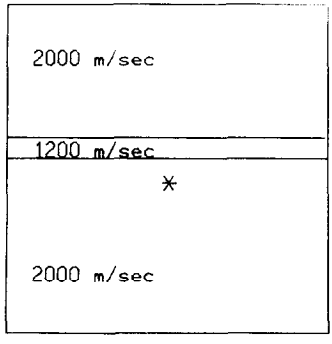

FIG. 6. The velocity field and the source in the two-dimensional acoustic problem.

regions, the absorbing boundary condition can be taylored and made highly effective.

To test the effectiveness of the absorbing boundary, two-dimensional accoustic wave propagation is considered. The problem consisted of a planar layer embedded in a uniform region with contrasting velocity (Fig. 6). A temporarily band limited point source was excited in the uniform region at a small distance from the layer. The calculations used a grid size of 64×64 with $dx = dy = 20$ m. The acoustic velocities were 2000 and 1200 m/sec for the exterior region and the layer, respectively. The density in this problem was constant. The point source had a Ricker wavelet time history with a highcut frequency of 40 Hz. The absorbing region surrounded the numerical mesh and had parameter values of $U_0 = 40\ \text{sec}^{-1}$ and $\alpha = 0.18\ \text{m}^{-1}$. Its effective width became fifteen grid points. The equations of motion (3.3) were solved numerically by the Fourier method [11], with a time integration based on the semi implicit method of Tal-Ezer [5]. For early times when the source term $S(x, y, t)$ was still active the time integration of (3.3) was carried out by second order differencing. (The semi implicit method applies directly only to homogeneous equations with no time dependent source terms).

Figure 7a–f shows amplitude snapshots at progressive times. As the figure indicates, when the waves impinge on the boundary region, they are eliminated without noticeable reflection or wraparound. For comparison, Figure 7g shows an amplitude snapshot for the same problem but without the absorbing boundaries. There the wraparound events clutter the picture completely.

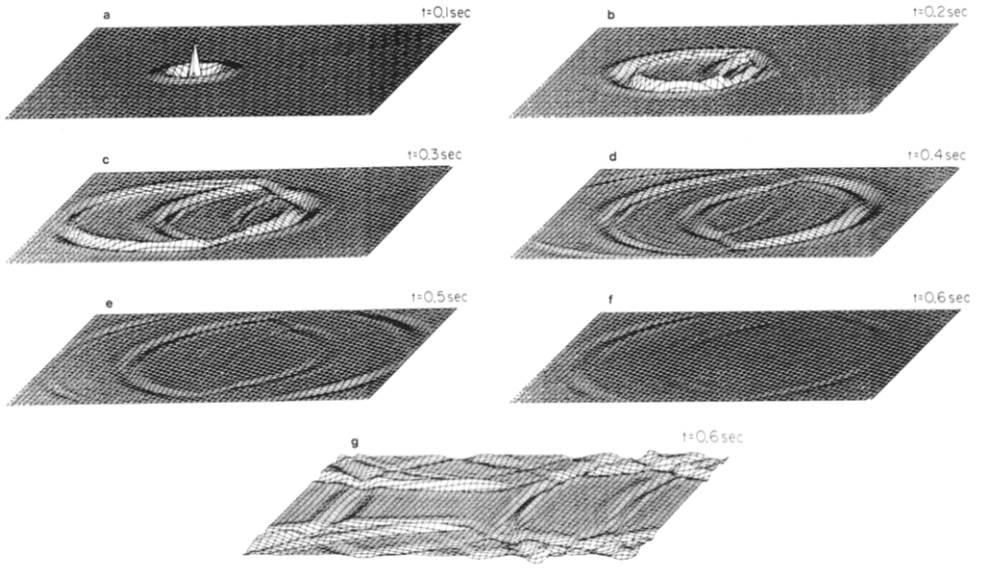

FIG. 7 (a)–(f) Amplitudes at progressive times for acoustic propagation with absorbing boundaries in a region containing a thin layer. (g) A snapshot at time $t = 0.6$ sec without absorbing boundaries.

IV. Conclusions

We have presented a numerical method for achieving absorbing boundaries for the Schrödinger equation and for the acoustic equation. These absorbing boundaries enable an expansion of the applicability of discrete methods to simulate physical phenomena.

An area of research in physical chemistry for which the absorbing boundary conditions may have special significance is in the direct simulation of time of flight experiments. In such experiments a pulsed beam of particles is scattered from a target which can be a surface or a laser beam or another beam of particles. Different inelastic scattering events reach the detectors at different times. By placing the absorbing boundary at the location of the detectors, a direct numerical simulation of these experiments can be achieved.

The second significant application is in the calculation of lifetimes and resonances or rates of desorption. These simulations require very long integration times and without the absorbing boundaries the wraparound or boundary reflection would clutter the picture completely.

Absorbing boundaries have already proven to be important in acoustic and elastic forward modeling for petroleum exploration. In effect the absorbing region allow the simulation in a finite mesh of wave propagation through the earth, obtaining semi-infinite space results. The importance of the scheme gains added significance in three-dimensional calculations for which boundary effects can be very pronounced and for which economical considerations induce the use of as small a grid as possible.

The method of this study for constructing absorbing boundary conditions is not based on specific equations and therefore it can also be applied to other types of wave propagation problems. Since it is not dependent on the Fourier method it can also be applied equally well to finite difference or finite element methods. The systematic approach presented for the calculation of reflection and transmission coefficients of the absorbing region, can aid in finding the optimal parameters of a given poblem.

APPENDIX: Derivation of Reflection and Transmission Coefficients for the One-Dimensional Acoustic Wave Equation

In this Appendix the generalized reflection and transmission coefficients for the 1-D acoustic propagation are derived. The derivation is based on considering a sinosoidal wave which impinges on a region with a variable amplitude reduction parameter $\gamma(X)$.

Consider again the modified acoustic wave equation, in one dimension with constant density,

$$\frac{\partial^2 p}{\partial t^2} = c^2 \frac{\partial^2 p}{\partial x^2} - 2\gamma \frac{\partial p}{\partial t} - \gamma^2 p, \tag{A.1}$$

in which c is constant and the variable γ differs from zero; only in the region $a \leqslant x \leqslant b$ and can assume arbitrary values there. A plane sinosoidal wave $\exp(i(wt-kx))$ in the region $x<a$ generates a reflected wave $R\exp(i(wt+kx))$ upon reflection at the boundary at $x=a$. The reflection coefficient R is generally complex. In the region $b<x$ only the transmitted wave $T\exp(i(wt-kx))$ propagates with T denoting the generalized transmission coefficient.

The calculation of the coefficients R and T can be performed with the propagator matrix method [12]. The region $a \leqslant x \leqslant b$ is divided into small intervals: $a = x0 < x1 < x2 < \cdots < Xn = b$. In each $x_l \leqslant x \leqslant x_{l+1}$ the parameter γ is approximated to be constant γ_l. Excluding the common factor $\exp(iwt)$, the solution to the modified acoustic wave equation in each interval 1 is given by

$$A_l^- \exp(-ik_l(x-x_l)) + B_l^- \exp(ik_l(x-x_l)), \tag{A.2}$$

or alternatively

$$A_l^+ \exp(-ik_l(x-x_{l+1})) + B_l^+ \exp(ik_l(x-x_{l+1})). \tag{A.3}$$

k_l is equal to $(w-i\gamma_l)/c$, whereas A_l^- or A_l^+ and B_l^- or B_l^+ are as yet undetermined coefficients which give amplitudes of waves traveling to the right and to the left, respectively. The coefficients A_l^- and B_l^- can be related to A_l^+ and B_l^+ by equating the amplitudes in (A.2) and (A.3) at the point $x = x_{l+1}$. This gives

$$A_l^+ = A_l^- \exp(-ik_l(x_{l+1}-x_l)), \tag{A.4}$$

$$B_l^+ = B_l^- \exp(ik_l(x_{l+1}+x_l)), \tag{A.5}$$

or in matrix notation

$$\begin{bmatrix} A_l^+ \\ B_l^+ \end{bmatrix} = \begin{bmatrix} \exp(-ik_l(x_{l+1}-x_l)) & 0 \\ 0 & \exp(ik_l(x_{l+1}-x_l)) \end{bmatrix} \begin{bmatrix} A_l^- \\ B_l^- \end{bmatrix}. \tag{A.6}$$

Equation (A.6) relates the amplitude coefficients in solutions which are, respectively, expanded from the left and from the right boundaries of the region $x_l \leqslant x \leqslant x_{l+1}$. In addition to relating coefficients within a region, a relation expressing A_{l+1}^-, B_{l+1}^- in terms of $A_l^+ B_l^+$ at a boundary separating two regions is required. This relation is obtained by requiring continuity of P and dp/dx on the boundary. Using (A.2) and (A.3) this gives

$$A_l^+ + B_l^+ = A_{l+1}^- + B_{l+1}^- \tag{A.7}$$

and

$$ik_l(-A_l^+ + B_l^+) = ik_{l+1}(-A_{l+1}^- + B_{l+1}^-). \tag{A.8}$$

Solving for A_{l+1}^- and B_{l+1}^- yields,

$$A_l^- = \frac{k_{l+1}+k_l}{2k_{l+1}} A^+ + \frac{k_{l+1}+k_l}{2k_{l+1}} B_l^- \tag{A.9}$$

and

$$B_{l+1}^- = \frac{k_{l+1}+k_l}{2k_{l+1}} B_l^+ + \frac{k_{l+1}+k_l}{2k_{l+1}} B_l^- . \tag{A.10}$$

A combination of (A.6) with (A.9) and (A.10) gives

$$\begin{bmatrix} A_{l+1}^- \\ B_{l+1}^- \end{bmatrix} = \begin{bmatrix} \frac{k_{l+1}+k_l}{2k_{l+1}} I^{i\Delta x_l k_l} & \frac{k_{l+1}+k_l}{2k_{l+1}} I^{-i\Delta x_l k_l} \\ \frac{k_{l+1}+k_l}{2k_{l+1}} I^{i\Delta x_l k_l} & \frac{k_{l+1}+k_l}{2k_{l+1}} I^{-i\Delta x_l k_l} \end{bmatrix} \begin{bmatrix} A_l^- \\ B_l^- \end{bmatrix} \tag{A.11}$$

with $\Delta x_l = x_{l+1} - x_l$. Equation (A.11) relates the amplitude coefficients in the lth region to the corresponding coefficients in the $l+1$ region. A successive application of (A.11) will yield a connection between the coefficients of any two regions. In particular since the coefficient at $x = x_0 = a$ and $x = x_n = b$ are respectively, given by

$$\begin{bmatrix} 1 \\ R \end{bmatrix} \quad \text{and} \quad \begin{bmatrix} Te^{i(w/c)b} \\ 0 \end{bmatrix},$$

we obtain

$$\begin{bmatrix} Te^{i(w/c)b} \\ 0 \end{bmatrix} = \begin{bmatrix} T_{11} & T_{12} \\ T_{21} & T_{22} \end{bmatrix} \begin{bmatrix} 1 \\ R \end{bmatrix}. \tag{A.12}$$

The matrix $(T_{11}\, T_{12}\, T_{21}\, T_{22})$ is formed from products of the individual matrices in (A.11) in each region. The generalized reflection coefficient can be solved from (A.12) giving

$$R = -T_{21}/T_{22} \tag{A.13}$$

and

$$T = \frac{T_{11}T_{22} - T_{12}T_{21}}{T_{22}} \cdot e^{-(iw/c)b}. \tag{A.14}$$

ACKNOWLEDGMENT

This work was supported by the Israel Academy of Science.

REFERENCES

1. C. CERJAN, D. KOSLOFF, R. KOSLOFF, AND RESHEF, *Geophysics* **50** (1985), 705.
2. J. LYSMER AND R. L. KUHLEMEYER, *J. Eng. Mech. Div. Proc. Amer. Soc. Civil Eng.* **95** (1969), 859.
3. R. CLAYTON AND B. ENQUIST, *Bull. Seismol. Soc. Amer.* **67** (6) (1977), 1529.
4. A. C. REYNOLDS, *Geophysics* **43** (6) (1978), 1099.
5. H. TAL-EZER AND R. KOSLOFF, *J. Chem. Phys.* **81** (1984), 3967.
6. M. D. FEIT, J. A. FLECK JR., AND A. STEIGER, *J. Comput. Phys.* **47** (1982), 412.
7. D. KOSLOFF AND R. KOSLOFF, *J. Comput. Phys.* **52** (1983), 35.
8. R. KOSLOFF AND D. KOSLOFF, *J. Chem. Phys.* **79** (1983), 1823.
9. L. D. LANDAU AND E. M. LIFSHITZ, "Quantum Mechanics," Pergamon, Oxford, 1965.
10. R. BISSLING AND R. KOSLOFF, *J. Comput. Phys.* **59** (1985), 136.
11. D. KOSLOFF AND E. BAYSAL, *Geophysics* **46** (1982), 854.
12. N. A. HASKELL, *Bull. Seismol. Soc. Amer.* **43** (1953), 17.
13. D. KOSLOFF, M. RESHEF, C. HSUING AND M. EDWARDS, *Geophysics* (1986), in press.